

# 博士學位論文

## 論文題名

(注：学位論文題名が英語の場合は和訳をつけること。)

Diffusional Kurtosis Imaging: optimization of  
the parameters considering diffusion time on  
diffusion quantification

拡散尖度画像法：撮像パラメータの最適化  
および拡散時間が与える影響

(西暦) 2015 年 1 月 7 日 提出

首都大学東京大学院

人間健康科学研究科 博士後期課程 人間健康科学専攻

放射線科学域

学修番号：12997606

氏名：福永 一星

(指導教員名： 妹尾 淳史 )

## (西暦) 2014 年度 博士後期課程学位論文要旨

学位論文題名 (注: 学位論文題名が英語の場合は和訳をつけること)

Diffusional Kurtosis Imaging: optimization of the parameters considering diffusion time on diffusion quantification

拡散尖度画像法: 撮像パラメータの最適化および拡散時間が与える影響

学位の種類: 博士 (放射線学)

首都大学東京大学院

人間健康科学研究科 博士後期課程 人間健康科学専攻 放射線科学域

学修番号 12997606

氏名: 福永 一星

(指導教員名: 妹尾 淳史)

注: 1 ページあたり 1,000 字程度 (英語の場合 300 ワード程度) で、本様式 1~2 ページ (A4 版) 程度とする。

【目的および背景】 拡散尖度画像法は従来の拡散テンソルとは異なる理論的背景による解析方法であり、正規分布を仮定しない拡散 (制限拡散) の評価が可能となる。また、 $b$  値  $3000[s/mm^2]$  以下で計算が可能のため、臨床応用が比較的容易である。本研究では、拡散尖度画像法を臨床に利用するための最適な  $b$  値、軸数、および拡散時間を検討した。また、拡散時間が拡散尖度の値に与える影響についてより詳細に検討した。

【方法】 対象は、健常ボランティア 4 名である。拡散尖度画像の撮像には 3T MRI 装置 (Philips 社製 Achieva) を使用し、以下の 3 つのプロトコルを撮像した。1.  $b$  値の検討、撮像条件: TR/TE 3000/99ms; スライス厚 5mm; 分解能  $2 \times 2 mm$ ; MPG 軸数 32 方向;  $b$  値  $0 \sim 7500[s/mm^2]$  (16 ステップ, 5 通りの組み合わせ)  
2. MPG 軸数の検討、撮像条件: TR/TE 8000/90ms; スライス厚 3mm; 分解能  $3 \times 3 mm$ ; MPG 軸数 6, 15, 20, 24, 28, 32 (6 種類);  $b$  値 0, 1000, 2000[s/mm<sup>2</sup>];  $\Delta/\delta$  44.1 / 34.5ms.  
3. 拡散時間の検討、撮像条件: TR/TE 5000/56-97ms; スライス厚 3mm; 分解能  $3 \times 3 mm$ ; MPG 軸数 30;  $b$  値 0, 1000, 2000[s/mm<sup>2</sup>];  $\delta/\Delta$  拡散時間 ( $\Delta-\delta/3$ ), 17.9/ 28.7/ 22.7, 13.3/ 45.3/ 40.9, 12.0/54.6/ 50.6, 10.8/ 65.8/ 62.2, 10.0/ 75.6/ 72.3 ms.; 加算回数 1, 2, 2, 2, 3

【結果および考察】 1.  $b$  値は高い値を使用した組み合わせになるほど、尖度の平均値が低下する傾向となった。先行報告によると、白質 (内包) は灰白質 (皮質) に比べて slow diffusion coefficient が有意に低いとされている。したがって、 $b=6000[s/mm^2]$  以上を使用した組み合わせにおいて灰白質の尖度の平均値が低下しなかったのは、 $b$  値を高くしても水分子の動きが遅い成分が比較的多いことによると考えられた。2. 軸数を増やすと尖度の平均値の標準偏差が低下した。6 軸ではその差が顕著にみられたが、15 軸以上では大きな差はなかった。3. 内包後脚の白質における神経線維と直交する方向の拡散係数は、拡散時間と正の相関関係を示した。髄鞘化が最も遅いといわれる側脳室三角部付近の白質で、平均拡散尖度の値は拡散時間と負の相関関係を示した。内包後脚では神経線維と垂直な方向で拡散を制限する構造が少ないため、垂直方向拡散尖度値と拡散時間が正の相関関係を示したと考えられる。また、側脳室三角部付近の白質では内包後脚などの白質とは異なり、拡散を制限する構造が比較的少ないため、平均拡散尖度値と拡散時間が負の相関関係を示したと考えられる。

【結論】  $b$  値、軸数、および拡散時間に関して検討し、全脳 15cm を 6 分 50 秒で撮像可能なプロトコルを提案することができた。 $b$  値は 0, 1000, and 2000[s/mm<sup>2</sup>], 軸数は 20 軸、拡散時間は  $\Delta/\delta$  45.3/13.3[ms] を最適な撮像条件とした。拡散尖度の値は拡散時間の影響を受ける可能性がある。

## CONTENTS

|   |      |
|---|------|
| Chapter1. Introduction .....                        | p.3  |
| 1.1 Back ground of the study.....                   | p.3  |
| 1.2 Purpose of the study.....                       | p.5  |
| Chapter2. Diffusion Tensor Imaging (DTI) .....      | p.6  |
| 2.1 Introduction (diffusion weighted imaging) ..... | p.6  |
| 2.2 Basic theory.....                               | p.8  |
| 2.3 Diffusion anisotropy.....                       | p.10 |
| Chapter3. Diffusion Kurtosis Imaging (DKI) .....    | p.13 |
| 3.1 Expectations, Moments, and Cumulants.....       | p.13 |
| 3.2 General properties about the kurtosis.....      | p.15 |
| 3.3 The signal intensity of the DKI.....            | p.17 |
| Chapter4. Optimization of the DKI parameters.....   | p.22 |
| 4.1 Introduction.....                               | p.22 |
| 4.2 Materials and Methods.....                      | p.23 |
| 4.3 Results.....                                    | p.27 |

|   |      |
|---|------|
| 4.4 Discussion.....   | p.33 |
| 4.5 Conclusion.....   | p.36 |
| Chapter5. Effects of Diffusion Time on Diffusion Quantification of<br>Diffusional Kurtosis Imaging..... | p.37 |
| 5.1 Introduction.....   | p.37 |
| 5.2 Materials and Methods.....  | p.38 |
| 5.3 Results.....  | p.40 |
| 5.4 Discussion.....   | p.44 |
| 5.5 Conclusion.....   | p.45 |
| Chapter6. Summary of the study.....   | p.46 |
| References.....   | p.47 |
| Acknowledgements.....   | p.53 |

# Chapter1. Introduction

## 1.1 Back ground of the study

Diffusion weighted imaging (DWI) is widely applied as a possible noninvasive biomarker for evaluating neural tissue in vivo. The diffusion of water through a biologic tissue provides image contrast that is depending on the molecular motion of water. The method of the DWI was introduced into clinical practice in the 1990s<sup>1)-3)</sup>. DWI technique can be used echo planar imaging (EPI), a fast imaging technique for DWI and DTI, and it is possible to detect the cerebral ischemia with imaging times ranging from a few seconds to 2 minutes<sup>4)</sup>.

Diffusion tensor imaging (DTI) is a relatively new MR technique enabling the in vivo examination of the white matter (WM) anisotropy in the human brain. The diffusion anisotropy is a parameter derived from directional distribution of diffusivity. The degrees of anisotropy have been shown to correlate with microstructural changes of neural tissues<sup>5)</sup>.

Diffusional kurtosis imaging (DKI) is highlighted as a new technique based on the

non-Gaussian water diffusion analysis<sup>6)</sup>. It is assumed that water diffusion in biological tissues is restricted. The non-Gaussian behavior of water molecules may provide useful information related to tissue structure and pathophysiology. Additionally, DKI may be useful for investigating abnormalities in tissues with isotropic structure, such as gray matter (GM)<sup>6)</sup>.

Many studies have been conducted using DKI technique to evaluate cerebral infraction, glioma, multiple sclerosis, Parkinson disease, and attention-deficit hyperactive disorder.<sup>4), 7)-10)</sup>. It is important to use DKI as a clinical tool for investigation of the imaging parameters in the healthy brain in vivo. In the DKI technique, it is preferable to acquire DKI datasets with multiple b value to minimize the fitting errors. However, the original protocol (6 b values and 30 MPG directions)<sup>6)</sup> needed more than 10 minutes for scanning time, which seemed to be too long for daily clinical use. Moreover, there are still few reports of the imaging parameter of DKI<sup>11), 12)</sup> compared with DTI or DWI<sup>13)-15)</sup>.

## 1.2 Purpose of the study

This study investigated the influence of imaging parameters on the measurement of mean kurtosis (MK). To find a suitable clinical setting of DKI, this study examined the b value, number of MPG direction, and diffusion time.

Furthermore, this study investigated the relationship between the diffusional kurtosis metrics and diffusion time.

## Chapter2. Diffusion Tensor Imaging (DTI)

### 2.1 Introduction (diffusion weighted imaging)

In the technique known as DWI, the diffusion of water through biological tissue provides image contrast that depends on the Brownian motion of water molecules. That random motion in the presence of a magnetic gradient results in MR signal loss.

Diffusion weighted SE- EPI can be achieved with a pair of diffusion gradients applied before and after the  $180^\circ$  RF pulse to dephase and remove signals caused by diffusing protons (Stejskal-Tanner method <sup>16)</sup> <sup>17)</sup>.

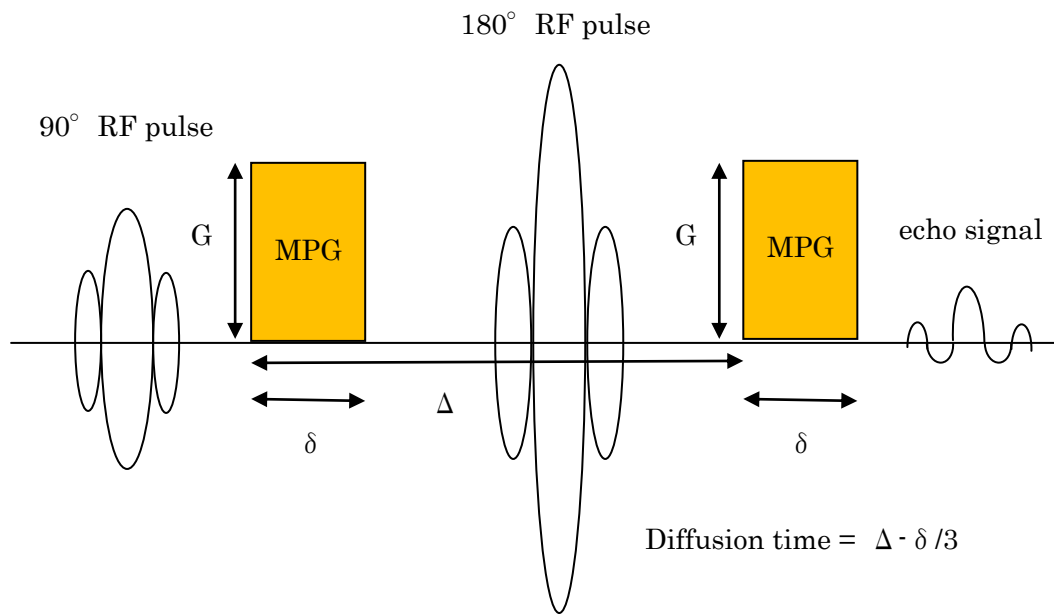


Figure 2-1. The spin-echo diffusion-weighted MRI sequence. The gradient duration is determined by  $\delta$ . The time between the two leading edges of diffusion gradient is determined by  $\Delta$ . From these two gradient parameters, the diffusion time is determined by  $\Delta - \delta/3$ .

## 2.2 Basic theory

The degree of diffusion weighting is described by the b value, which is determined by the type of motion probing gradient (MPG). In other words, the b value is determined by the gradient strength ( $G$ ), duration ( $\delta$ ), and the time between the two leading edges of diffusion gradient ( $\Delta$ ):

$$b \text{ value} = \gamma^2 G^2 \delta^2 \left( \Delta - \frac{\delta}{3} \right) \quad [1]$$

where  $\gamma$  is the gyromagnetic ratio<sup>18), 19)</sup>. The diffusion time is  $\Delta - \delta / 3$  (Fig. 2-1).

The following formula describes the relationship between the signal intensity of the diffusion-weighted MR image and the other parameters.

$$S = S_0 e^{-b(ADC)} \quad [2]$$

Where  $S_0$  is the signal value without the gradient<sup>18), 19)</sup>.

Diffusion can be fully characterized by the symmetric  $3 \times 3$  diffusion tensor matrix  $D$ :

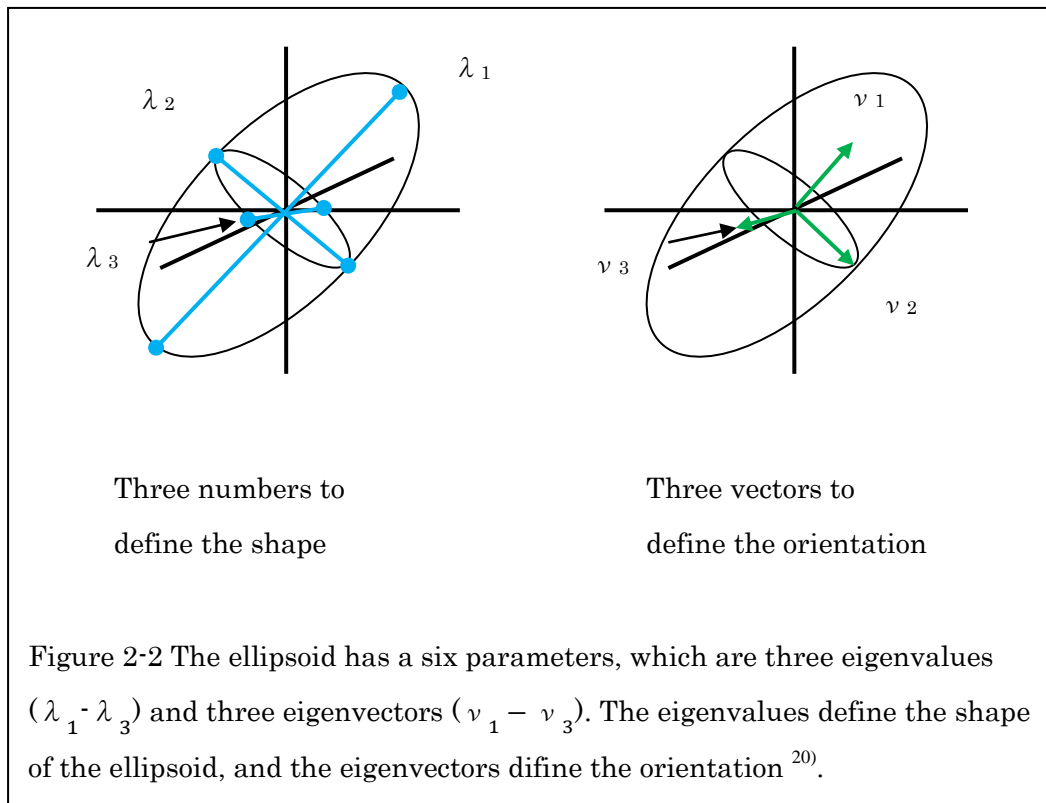
$$D = \begin{bmatrix} D_{xx} & D_{xy} & D_{xz} \\ D_{yx} & D_{yy} & D_{yz} \\ D_{zx} & D_{zy} & D_{zz} \end{bmatrix} \quad [3]$$

where  $D_{xx}$ ,  $D_{yy}$ , and  $D_{zz}$  relate the diffusional fluxes to the gradients in the  $x$ ,  $y$ , and  $z$  directions (diagonal elements). By performing a similarity transform, the nondiagonal elements in the matrix are exempted. Thus, the  $3 \times 3$  diffusion tensor has nine elements,

but there are enough six independent elements to calculate the diffusion ellipsoid <sup>17), 18)</sup>.

The shape and orientation of the 3D ellipsoid is described by these six parameters, and

the determination of these six parameters is the target of DTI (Fig. 2-2) <sup>18), 20)</sup>.



## 2.3 Diffusion anisotropy

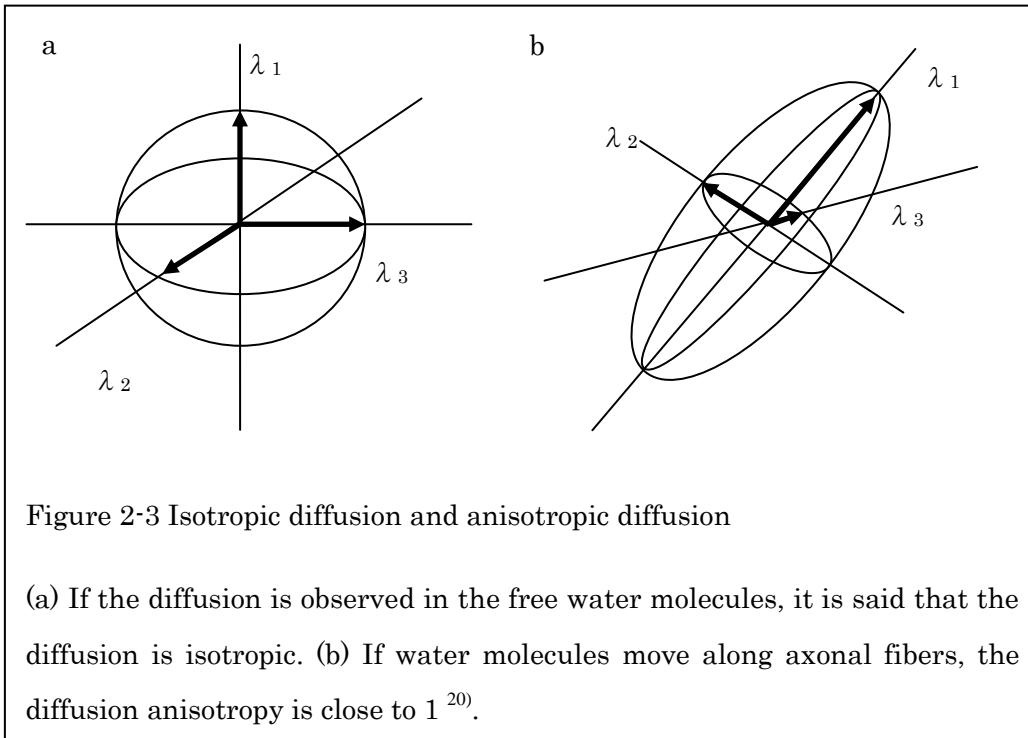
A tensor characterizes diffusion in the brain not only by a single apparent diffusion coefficient (ADC) but by three diffusion eigenvalues ( $\lambda_1, \lambda_2, \lambda_3$ ) describing diffusion along three eigenvectors ( $v_1, v_2, v_3$ ). Axial diffusivity is defined by the axial eigenvalue ( $\lambda_1$ ) to the main WM tract, and radial diffusivity is defined by the radial eigenvalue ( $\lambda_{23}$ : average value of  $\lambda_2$  and  $\lambda_3$ ).

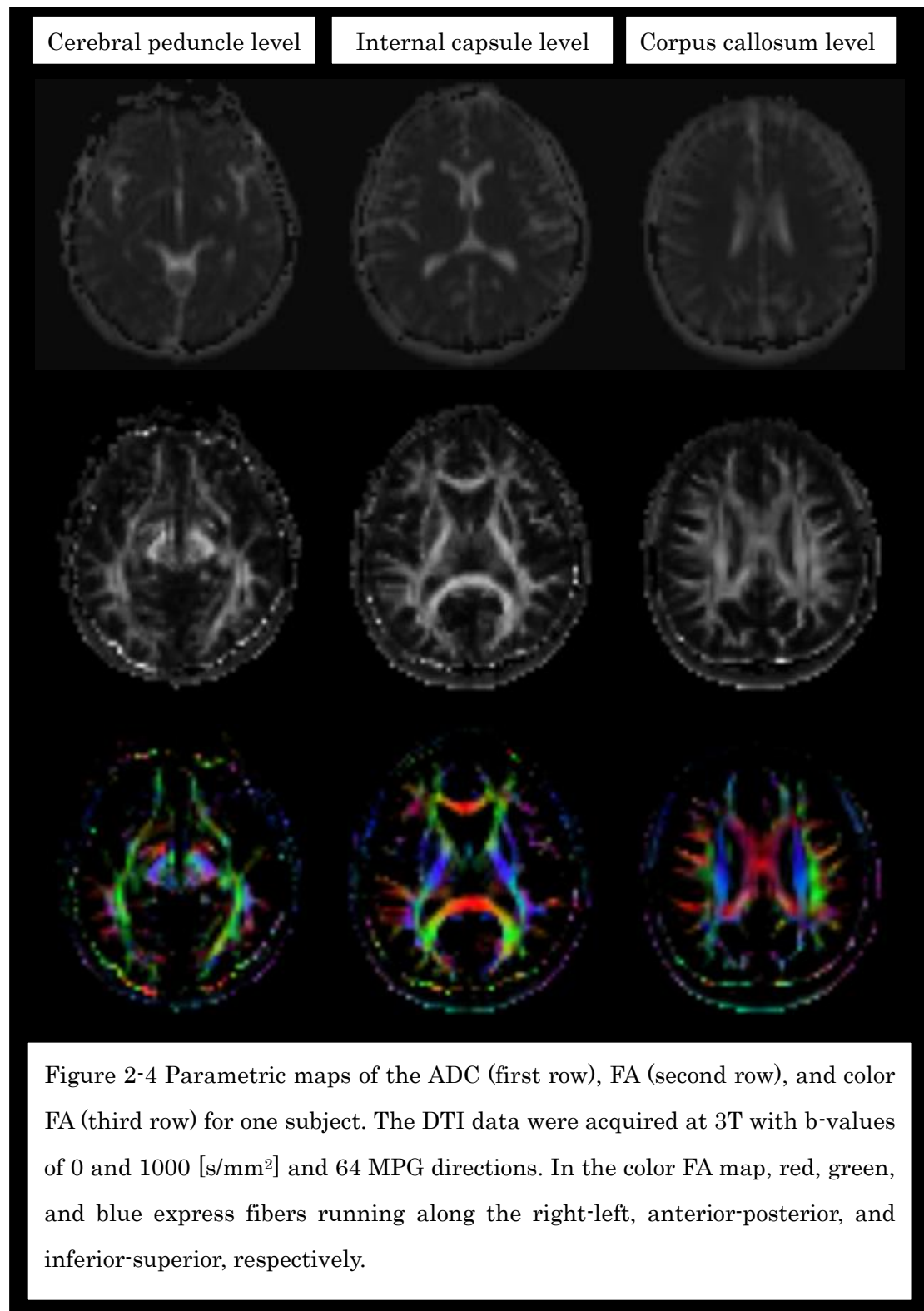
The ADC and FA were calculated by following formula:

$$ADC = \frac{\lambda_1 + \lambda_2 + \lambda_3}{3} \quad [4]$$

$$FA = \sqrt{\frac{3}{2}} \sqrt{\frac{(\lambda_1 - \lambda_2)^2 + (\lambda_1 - \lambda_3)^2 + (\lambda_2 - \lambda_3)^2}{(\lambda_1 + \lambda_2 + \lambda_3)^2}} \quad [5]$$

The ADC value is the diffusion magnitude indices, which is irrelevant to the diffusion directions. The FA value is typical of the strength as diffusion anisotropy, and it is scaled from 0 (isotropic) to 1 (anisotropic) (Fig. 2-3). The ADC, FA, and color FA maps are shown below (Fig. 2-4) <sup>21), 22)</sup>.





## Chapter3. Diffusional Kurtosis Imaging (DKI)

### 3.1 Expectations, Moments, and Cumulants

The exact probability density function (PDF) is usually unknown. However, one can use instead expectations of some functions for performing useful analysis and processing. A great advantage of expectations is that they can be estimated directly from the data, although they are formally defined in the density function.

Let  $g(x)$  signify any variable derived from the probabilistic vector  $x$ . The variable  $g(x)$  may be a scalar, vector, or even a matrix. The expectation of  $g(x)$  is signified by  $E\{g(x)\}$ , and is given by the following formula.

$$E\{g(x)\} = \int_{-\infty}^{\infty} g(x) p_x(x) dx \quad [6]$$

Where  $p_x(x)$  is the PDF. If  $g(x) = x$ , formula (5) equals to the expectation  $E\{x\}$  of  $x$ .

Moments of a probabilistic vector  $x$  are typical expectations used to feature it. The first moment of a probabilistic vector  $x$  is especially called the mean vector  $m_x$  of  $x$ . It is given as the expectation of  $x$ :

$$m_x = E\{x\} = \int_{-\infty}^{\infty} x p_x(x) dx \quad [7]$$

Next, we present the general definition of cumulants. Hypothesize that  $x$  is a real-valued, zero-mean, continuous scalar probabilistic variable with PDF.

The first characteristic function  $\varphi(\omega)$  of  $x$  is given as the continuous Fourier transform of the PDF:

$$\varphi(\omega) = E\{\exp(j\omega x)\} = \int_{-\infty}^{\infty} \exp(j\omega x) p_x(x) dx \quad [8]$$

All probability distribution is uniquely specified by its characteristic function, and vice versa. Now, we expand the characteristic function  $\varphi(\omega)$  into its Taylor series:

$$\varphi(\omega) = \int_{-\infty}^{\infty} \left( \sum_{k=0}^{\infty} \frac{x^k (j\omega)^k}{k!} \right) p_x(x) dx = \sum_{k=0}^{\infty} E\{x^k\} \frac{(j\omega)^k}{k!} \quad [9]$$

Therefore, the coefficient terms of formula (8) are moments  $E\{x^k\}$  of  $x$ . For that reason, the characteristic function  $\varphi(\omega)$  is also called the moment generating function.

It is often desirable to use the second characteristic function  $\varphi(\omega)$  of  $x$ , or cumulant generating function, this function is given by the natural logarithm of the first characteristic function:

$$\varphi(\omega) = \ln(\varphi(\omega)) = \ln(E\{\exp(j\omega x)\}) \quad [10]$$

The cumulants  $\kappa_k$  of  $x$  are given in a similar way to the respective moments as the

coefficients of the Taylor series expansion of the second characteristic function:

$$\varphi(\omega) = \sum_{k=0}^{\infty} \kappa_k \frac{(j\omega)^k}{k!} \quad [11]$$

For a zero mean probabilistic variable  $x$ , the first four cumulants are

$$\kappa_1 = 0, \kappa_2 = E\{x^2\}, \kappa_3 = E\{x^3\}, \kappa_4 = E\{x^4\} - 3[E\{x^2\}]^2 \quad [12]$$

Thus the first three cumulants are equal to the respective moments, and the fourth cumulant  $\kappa_4$  is the kurtosis.

We show the respective expressions for the cumulants when the mean  $E\{x\}$  of  $x$  is nonzero <sup>23)</sup>.

$$\kappa_1 = E\{x\} \quad [13]$$

$$\kappa_2 = E\{x^2\} - [E\{x\}]^2 \quad [14]$$

$$\kappa_3 = E\{x^3\} - 3E\{x^2\}E\{x\} + 2[E\{x\}]^3 \quad [15]$$

$$\kappa_4 = E\{x^4\} - 3[E\{x^2\}]^2 - 4E\{x^3\}E\{x\} + 12E\{x^2\}[E\{x\}]^2 - 6[E\{x\}]^4 \quad [16]$$

### 3.2 General properties about the kurtosis

In practice, higher than fourth order moments and statistics are used seldom, so we discuss more specifically fourth-order moments. The fourth-order statistics called the

kurtosis has some useful properties, and it is important in independent component analysis and blind source separation.

In the zero-mean, kurtosis is given in formula:

$$kurt(x) = E\{x^4\} - 3[E\{x^2\}]^2 \quad [17]$$

The normalized kurtosis can be used instead:

$$\kappa_4 = \frac{E\{x^4\}}{[E\{x^2\}]^2} - 3 \quad [18]$$

In addition, important characteristics of kurtosis are that it is the simplest statistical quantity for indicating the nongaussianity of a statistical variable. If  $x$  has a gaussian distribution, its kurtosis is zero. And a distribution having zero kurtosis is called mesokurtic in statistical.

Generally, the distributions having a negative kurtosis are called subgaussian (or platykurtic in statistics). On the other hand, the distributions having a positive kurtosis are called supergaussian (or leptokurtic in statistics). Subgaussian tend to be flatter than the gaussian PDF, or multimodal. A typical supergaussian has a slender peak and longer tails than the gaussian PDF.

Kurtosis is often used as a measure of the nongaussianity of a probabilistic variable

or signal, but some caution must be needed. The reason is that the kurtosis of a supergaussian signal may have a large positive value, which maximum is infinity in principle. However, the kurtosis of a subgaussian signal is finite, which the minimum possible value is  $-2$  <sup>23)</sup>.

### 3.3 The signal intensity of the DKI

The kurtosis is a statistics value showing the degree of deviation from a normal distribution, and parametric maps of  $K_{app}$  were created by using the formula.

$$S_{exp} = \left\{ \eta^2 + \left[ S_0 \exp \left( -bD_{app} + \frac{1}{6} b^2 D_{app}^2 K_{app} \right) \right]^2 \right\}^{\frac{1}{2}} \quad [19]$$

Where  $\eta$  is the Rician noise,  $D_{app}$  is the apparent diffusion coefficient for the given direction,  $K_{app}$  is the apparent kurtosis coefficient and is a dimensionless parameter <sup>6)</sup>.

The diffusion tensor has  $3^2 = 9$  elements, but because of symmetry only six are independent. The kurtosis has  $3^4 = 81$  elements, but because of symmetry only 15 are independent. With these two tensors,  $K_{app}$  in an arbitrary direction is calculated by following formula.

$$K_{app} = \frac{MD^2}{D_{app}^2} \sum_{i=x,y,z} \sum_{j=x,y,z} \sum_{k=x,y,z} \sum_{l=x,y,z} n_i n_j n_k n_l W_{ijkl} \quad [20]$$

Where  $MD$  is mean diffusivity,  $n_i n_j n_k n_l$  is elements of the direction vector  $n$ , and  $W$  is elements of the diffusion kurtosis <sup>11), 12)</sup>.

For a special case of three b-values, the simple closed-form is calculated by following formula.

$$D = \frac{(b_3 + b_1)D^{(12)} - (b_2 + b_1)D^{(13)}}{b_3 - b_2} \quad [21]$$

$$K = 6 \frac{D^{(12)} - D^{(13)}}{(b_3 - b_2)D^2} \quad [22]$$

$$D^{(12)} = \frac{\ln\left[\frac{S(b_1)}{S(b_2)}\right]}{b_2 - b_1}, D^{(13)} = \frac{\ln\left[\frac{S(b_1)}{S(b_3)}\right]}{b_3 - b_1} \quad [23]$$

Where  $D^{(12)}$  and  $D^{(13)}$  are the DTI estimates of the diffusion coefficient for the b-values pairs of  $(b_1, b_2)$  and  $(b_1, b_3)$ , respectively <sup>12)</sup>.

It is desirable to acquire DKI datasets with multiple b value to minimize the fitting errors.

The mean kurtosis, axial kurtosis, and radial kurtosis maps are shown below (Fig. 3-1).

Mean kurtosis is the qualitative estimation of overall diffusional heterogeneity in tissue, independent of direction. Axial kurtosis is the qualitative estimation of diffusional heterogeneity along principal direction, parallel with WM fiber orientation. Radial kurtosis is qualitative estimation of diffusional heterogeneity perpendicular to principal

direction, perpendicular to WM fiber orientation <sup>4)</sup>.

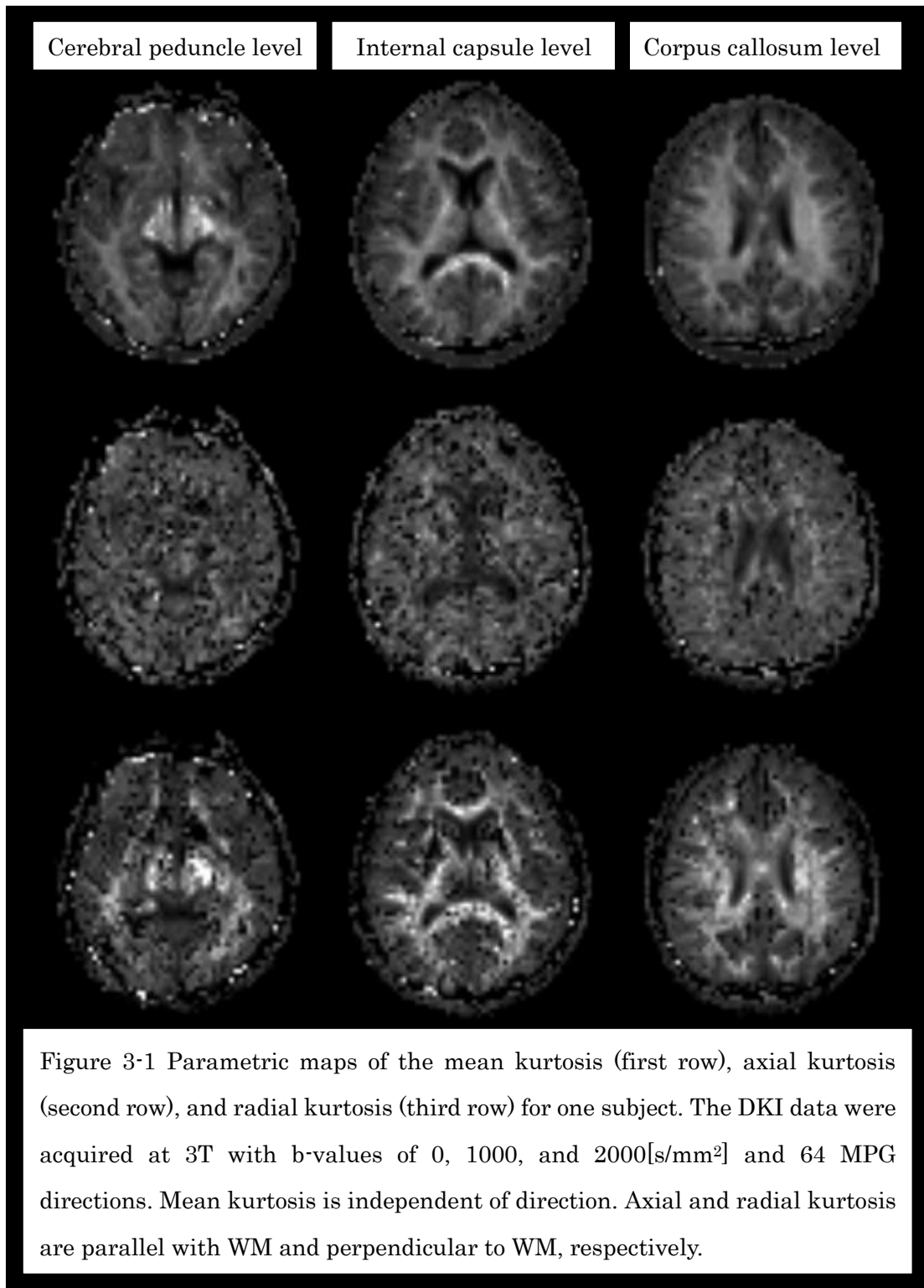
#### Advantages of DKI (compared with DTI)

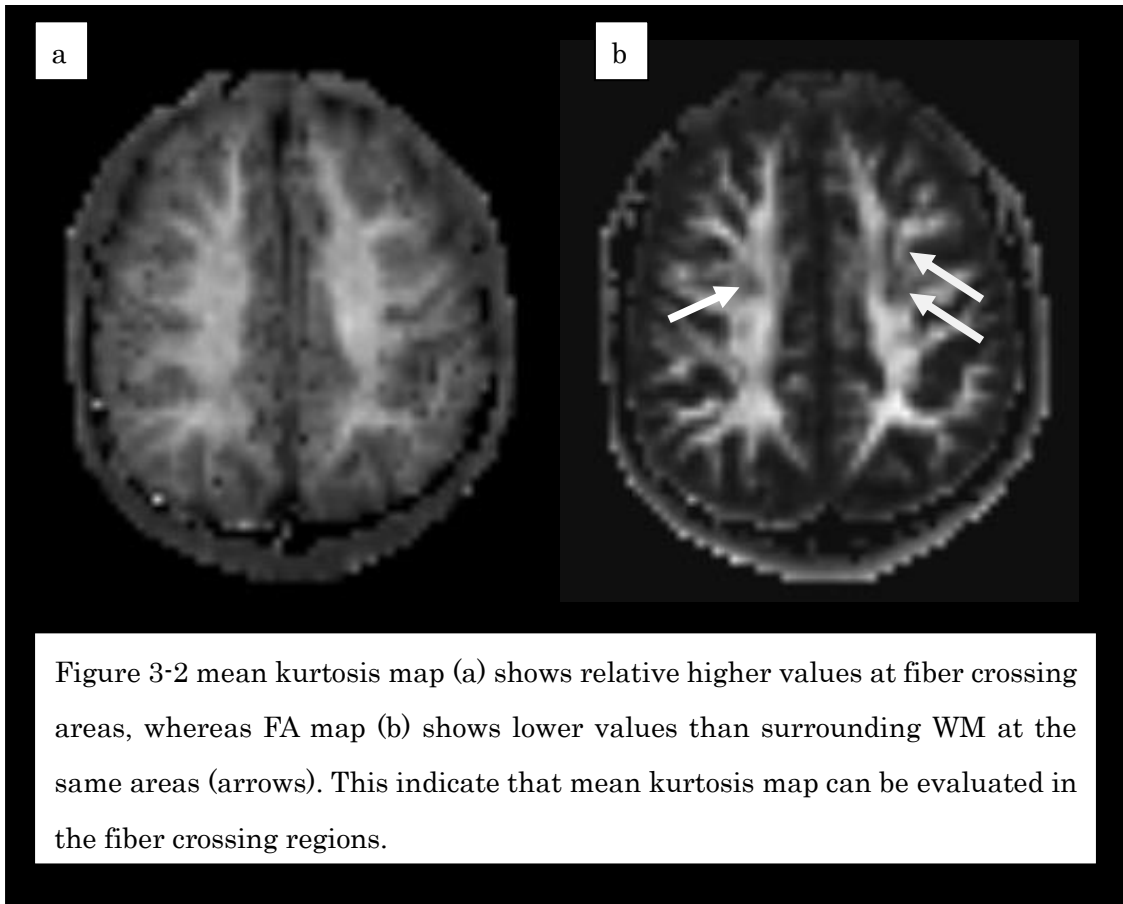
1. The main advantage of the DKI approach is that it is relatively model-free.

Therefore, DKI is not needed to calculate complicated mathematical models <sup>24)</sup>.

2. DKI does not depend on spatially oriented tissue structures, so DKI can be used to feature both GM and WM.

3. DKI technique can be used to resolve crossing fiber tracts, whereas the DTI cannot (Fig. 3-2) <sup>8)</sup>.





## Chapter4. Optimization of the DKI parameters

### 4.1 Introduction

DWI is widely applied as a possible noninvasive biomarker for evaluating neural tissue *in vivo*. DWI can be used with EPI, a fast imaging technique for DWI and DTI, through which it is possible to detect cerebral ischemia with imaging times ranging from a few seconds to 2 minutes <sup>4)</sup>. Diffusion tensor imaging is a MRI technique enabling *in vivo* examination of WM anisotropy in the human brain. Diffusion anisotropy is a parameter derived from the directional distribution of diffusivity, and the degrees of anisotropy have been shown to correlate with microstructural changes in neural tissues <sup>6)</sup>.

Diffusional kurtosis imaging (DKI) has been highlighted as a new technique based on non-Gaussian water diffusion analysis <sup>6)</sup>. It is assumed that water diffusion in biological tissues is restricted. The non-Gaussian behavior of water molecules may provide useful information related to tissue structure and pathophysiology <sup>2)</sup>. Many studies have been conducted with DKI for evaluation of cerebral infarction, glioma,

multiple sclerosis, Parkinson disease, attention-deficit hyperactive disorder, and spondylotic myelopathy <sup>4), 7-10), 25), 26)</sup>. It is important to use DKI as a clinical tool for investigation of the imaging parameters in the healthy brain in vivo. In the DKI technique, it is preferable to acquire DKI datasets with multiple b value to minimize the fitting errors. However, the original protocol (six b values and 30 motion-probing gradient (MPG) directions) <sup>6)</sup> requires more than 10 minutes of scanning time, which is regarded as being too long for daily clinical use. Moreover, until now, few reports have been conducted on the imaging parameters of DKI <sup>11), 12)</sup> compared with those of diffusion tensor imaging and DWI <sup>13)-15)</sup>.

## 4.2 Materials and Methods

Four normal healthy subjects (age range 21–24 years, mean age 22.5 years) participated in the study. This study was approved by the institutional review board of Tokyo Metropolitan University (No. 14053) and Juntendo University School of Medicine (No. 351). Written informed consent was obtained from all participants and their relatives. All DKI data were acquired on a clinical 3T-MRI scanner (Philips Medical

Systems, Best, The Netherlands) with use of three study protocols as follows:

Protocol 1. Repetition time/echo time (TR/TE), 3000/99 ms; slice thickness, 5 mm; resolution, 2×2 mm; MPG directions, 32; b values, 0–7500 s/mm<sup>2</sup> (16 steps, refer to Table 4-1); The time between the two leading edges of the diffusion gradient ( $\Delta$ ) and the gradient length ( $\delta$ ) were 49.1 and 39.1 ms. The total scan time was approximately 48 minutes 18 seconds.

Protocol 1 used three b values, b = 0, 1000, and 2000 s/mm<sup>2</sup>, as proposed in 2010 (Jensen et al.)<sup>12)</sup>. Protocol 2 used six b values, b = 0, 500, 1000, 1500, 2000, 2500 s/mm<sup>2</sup>, as the original protocol, which was proposed in 2005 (Jensen et al.)<sup>6)</sup>. For Protocols 3 to 5, this study prepared a combination that used six higher b values than those of Protocol 2, in order to compare these two protocols with MK values. Protocol 3 used b = 0, 500, 1000, 2000, 3000, and 5000 s/mm<sup>2</sup>. Protocol 4 used b = 0, 1000, 3000, 5000, 6000, and 7000 s/mm<sup>2</sup>. Protocol 5 used b = 0, 5500, 6000, 6500, 7000, and 7500 s/mm<sup>2</sup>.

Protocol 2. TR/TE, 8000/90 ms; slice thickness, 3 mm; resolution, 3×3 mm; MPG directions, 6-32 (6 variations, refer to Table 4-2); b values, 0, 1000, 2000 s/mm<sup>2</sup>;  $\Delta/\delta$ , 44.1/34.5 ms. The total scan time was approximately 44 minutes 22 seconds. The scan

time for 6 MPG directions was 2 minutes 26 seconds, for 15 MPG directions was 5 minutes 27 seconds, for 20 MPG directions was 7 minutes 7 seconds, for 24 MPG directions was 8 minutes 27 seconds, for 28 MPG directions was 9 minutes 48 seconds, and for 32 MPG directions was 11 minutes 7 seconds. Jones et al. applied the theory of electrostatic repulsion algorithm to calculate optimal gradient directions <sup>27)</sup>. The protocol of 20, 24, 28 MPG directions is applied their algorithm. To study the MPG direction, this study evaluated the standard deviation (SD) of the MK value in WM and GM.

Protocol 3. TR/TE, 8000/56–104 ms; slice thickness, 3 mm; resolution, 3×3 mm; MPG directions, 20; b values, 0, 1000, 2000 s/mm<sup>2</sup>;  $\Delta/\delta$ , 28.7–83.1/9.5–34.5 ms (6 variations, refer to Table 4-3). Total scan time was approximately 48 minutes 26 seconds.

Statistical analysis was performed with Scientific Package for Social Sciences, version 20 (SPSS, Chicago, Illinois). This study used Pearson correlation to investigate the relationships between MK and diffusion time, and the relationships between the signal-to-noise ratio (SNR) and diffusion time. This study assumed that, under ideal conditions, the cerebrospinal fluid (CSF) would have a Gaussian distribution. Thus, the

MK value of the CSF would be close to zero. This study supposed that a lower MK value would improve the diffusion precision.

All data were calculated for all diffusion metric maps such as FA, ADC, and MK, with the software dTV.II.FZR <sup>28)</sup>.

The volumes of interest (VOIs) were placed on the PLIC (Fig.4-1A), corpus callosum (CC) (Fig.4-1B), thalamus (Fig.4-1C) , and anterior horn of the lateral ventricle (as CSF) (Fig.4-1 D). The size of VOIs was 19 voxels.

To study diffusion time, this study placed the regions of interest (ROIs) in the globus pallidus and the extra-cranial background region by using MRICro (free software), in order to measure the SNR. For DKI, the globus pallidus has been shown to be a useful region for the testing SNR at 3T <sup>12)</sup>. The SNR was defined as the mean signal intensity in the globus pallidus and the standard deviation of the noise in the extra-cranial background region <sup>29)</sup>. In studying the VOIs and ROIs, the VOIs and ROIs were saved and used for every subject and every protocol.

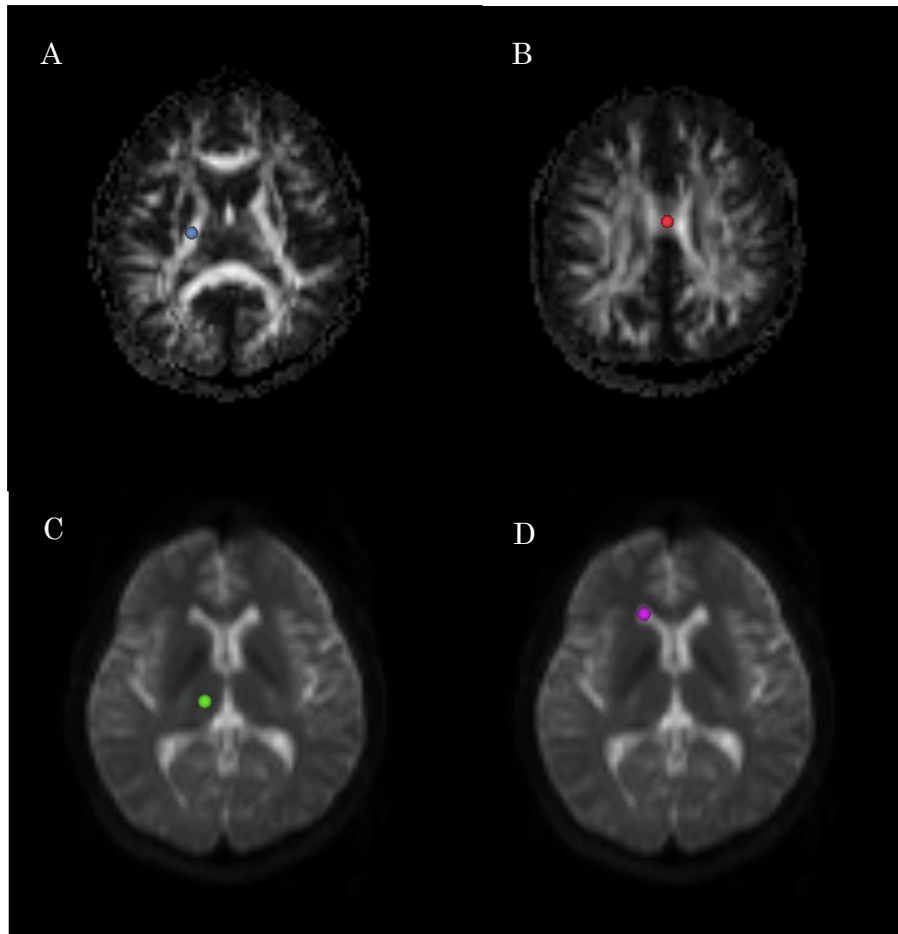


Fig. 4-1 Volumes of interest (VOIs) showed on FA map (A, B) and T2-weighted image without motion probing gradient (C, D). A Posterior limb of the internal capsule, B corpus callosum, C thalamus, D anterior horn of the lateral ventricle

### 4.3 Results

Result 1. The FA, ADC, and MK values were lower in the WM and GM with higher b values; this tendency was seen in the combination in which b values were above 6000 s/mm<sup>2</sup> (Protocols 4 and 5) in the ADC (Table 4-1, Fig. 4-2).

Result 2. The FA and ADC values did not differ in the number of MPG directions. However, there was a remarkable difference in the SD of the MK values (Table 4-2).

Result 3. The MK values were significantly higher with use of a longer diffusion time in the PLIC (p=0.003, r=0.924) and thalamus (p=0.005, r=0.903), whereas the MK values for the CSF (p=0.001, r=-0.976) were significantly lower with use of a longer diffusion time. The SNR decreased significantly with diffusion time (p=0.001, r=-0.978) (Table 4-3, Fig. 4-3).

Table 4-1 Protocol of b values and Diffusional Kurtosis Imaging Metrics

|                               | Protocol No. <sup>a</sup> | Posterior limb of the internal capsule | Corpus callosum | Thalamus  | Cerebrospinal fluid |
|-------------------------------|---------------------------|--|-----------------|-----------|---------------------|
| diffusion tensor analysis     |                           |  |                 |           |                     |
| FA                            | 1                         | 0.75±0.08                              | 0.75±0.06       | 0.33±0.06 | 0.13±0.04           |
|                               | 2                         | 0.74±0.07                              | 0.77±0.05       | 0.32±0.06 | 0.12±0.04           |
|                               | 3                         | 0.73±0.09                              | 0.76±0.05       | 0.29±0.06 | 0.11±0.04           |
|                               | 4                         | 0.70±0.09                              | 0.72±0.05       | 0.30±0.05 | 0.11±0.05           |
|                               | 5                         | 0.66±0.09                              | 0.71±0.03       | 0.24±0.05 | 0.12±0.05           |
| ADC<br>[mm <sup>2</sup> /s]   | 1                         | 0.58±0.03                              | 0.84±0.14       | 0.66±0.14 | 1.90±0.21           |
|                               | 2                         | 0.58±0.04                              | 0.78±0.08       | 0.68±0.18 | 1.88±0.17           |
|                               | 3                         | 0.51±0.02                              | 0.71±0.08       | 0.64±0.17 | 1.64±0.13           |
|                               | 4                         | 0.41±0.02                              | 0.56±0.07       | 0.48±0.07 | 1.11±0.09           |
|                               | 5                         | 0.31±0.02                              | 0.38±0.02       | 0.38±0.03 | 0.66±0.04           |
| diffusional kurtosis analysis |                           |  |                 |           |                     |
| MK                            | 1                         | 1.22±0.15                              | 1.04±0.13       | 0.91±0.11 | 0.465±0.068         |
|                               | 2                         | 1.02±0.11                              | 1.02±0.09       | 0.71±0.09 | 0.453±0.055         |
|                               | 3                         | 0.89±0.05                              | 0.76±0.05       | 0.62±0.06 | 0.363±0.028         |
|                               | 4                         | 0.85±0.05                              | 0.66±0.05       | 0.63±0.05 | 0.342±0.025         |
|                               | 5                         | 0.72±0.06                              | 0.58±0.05       | 0.56±0.04 | 0.334±0.024         |

a. Each protocol number contains the following b values [s/mm<sup>2</sup>]:

Protocol 1: 0, 1000, and 2000

Protocol 2: 0, 500, 1000, 1500, 2000, and 2500

Protocol 3: 0, 500, 1000, 2000, 3000, and 5000

Protocol 4: 0, 1000, 3000, 5000, 6000, and 7000

Protocol 5: 0, 5500, 6000, 6500, 7000, and 7500

Uncertainties indicate standard deviation.

Table 4-2 MPG Directions and Diffusional Kurtosis Imaging Metrics

|                               | Motion Probing Gradient | Posterior limb of the internal capsule | Corpus callosum | Thalamus        | Cerebrospinal fluid |
|-------------------------------|-------------------------|--|-----------------|-----------------|---------------------|
| diffusion tensor analysis     |                         |  |                 |                 |                     |
| FA                            | 6                       | $0.65 \pm 0.15$                        | $0.66 \pm 0.14$ | $0.37 \pm 0.11$ | $0.22 \pm 0.12$     |
|                               | 15                      | $0.63 \pm 0.16$                        | $0.63 \pm 0.13$ | $0.35 \pm 0.11$ | $0.17 \pm 0.11$     |
|                               | 20                      | $0.61 \pm 0.16$                        | $0.62 \pm 0.15$ | $0.29 \pm 0.08$ | $0.15 \pm 0.11$     |
|                               | 24                      | $0.59 \pm 0.16$                        | $0.61 \pm 0.17$ | $0.29 \pm 0.06$ | $0.15 \pm 0.11$     |
|                               | 28                      | $0.60 \pm 0.16$                        | $0.62 \pm 0.16$ | $0.28 \pm 0.08$ | $0.16 \pm 0.12$     |
|                               | 32                      | $0.63 \pm 0.17$                        | $0.67 \pm 0.15$ | $0.29 \pm 0.08$ | $0.17 \pm 0.13$     |
| ADC<br>[mm <sup>2</sup> /s]   | 6                       | $0.65 \pm 0.06$                        | $1.02 \pm 0.22$ | $0.69 \pm 0.09$ | $2.24 \pm 0.36$     |
|                               | 15                      | $0.63 \pm 0.05$                        | $1.02 \pm 0.24$ | $0.69 \pm 0.08$ | $2.22 \pm 0.37$     |
|                               | 20                      | $0.63 \pm 0.05$                        | $0.97 \pm 0.24$ | $0.71 \pm 0.08$ | $2.22 \pm 0.37$     |
|                               | 24                      | $0.63 \pm 0.06$                        | $0.99 \pm 0.25$ | $0.73 \pm 0.11$ | $2.20 \pm 0.39$     |
|                               | 28                      | $0.62 \pm 0.05$                        | $0.98 \pm 0.25$ | $0.73 \pm 0.13$ | $2.08 \pm 0.38$     |
|                               | 32                      | $0.63 \pm 0.05$                        | $0.99 \pm 0.25$ | $0.72 \pm 0.14$ | $2.07 \pm 0.39$     |
| diffusional kurtosis analysis |                         |  |                 |                 |                     |
| MK                            | 6                       | $1.21 \pm 0.32$                        | $1.07 \pm 0.31$ | $0.94 \pm 0.17$ | $0.43 \pm 0.24$     |
|                               | 15                      | $1.26 \pm 0.21$                        | $0.97 \pm 0.26$ | $0.99 \pm 0.14$ | $0.44 \pm 0.34$     |
|                               | 20                      | $1.25 \pm 0.19$                        | $1.13 \pm 0.26$ | $0.90 \pm 0.13$ | $0.49 \pm 0.16$     |
|                               | 24                      | $1.21 \pm 0.18$                        | $1.10 \pm 0.31$ | $0.94 \pm 0.13$ | $0.44 \pm 0.17$     |
|                               | 28                      | $1.28 \pm 0.19$                        | $1.06 \pm 0.28$ | $0.97 \pm 0.13$ | $0.48 \pm 0.20$     |
|                               | 32                      | $1.28 \pm 0.16$                        | $0.99 \pm 0.24$ | $0.97 \pm 0.12$ | $0.48 \pm 0.18$     |

Uncertainties indicate standard deviation.

Table 4-3 Diffusion Time and Diffusional Kurtosis Imaging Metrics

| Diffusion time <sup>a</sup> / TE [ms] | Posterior limb of the internal capsule | Corpus callosum | Thalamus    | Cerebrospinal fluid | SNR      |
|---------------------------------------|--|-----------------|-------------|---------------------|----------|
| 22.7 / 56                             | 1.14 ± 0.17                            | 1.21 ± 0.15     | 0.87 ± 0.11 | 0.47 ± 0.04         | 276 ± 48 |
| 40.9 / 70                             | 1.21 ± 0.18                            | 1.19 ± 0.23     | 0.88 ± 0.12 | 0.46 ± 0.05         | 208 ± 49 |
| 50.6 / 78                             | 1.20 ± 0.21                            | 1.22 ± 0.09     | 0.88 ± 0.11 | 0.44 ± 0.05         | 211 ± 54 |
| 62.2 / 88                             | 1.23 ± 0.21                            | 1.19 ± 0.15     | 0.92 ± 0.13 | 0.42 ± 0.06         | 162 ± 51 |
| 72.3 / 97                             | 1.30 ± 0.20                            | 1.09 ± 0.19     | 0.92 ± 0.14 | 0.41 ± 0.05         | 145 ± 67 |
| 79.9 / 104                            | 1.37 ± 0.22                            | 1.19 ± 0.12     | 0.96 ± 0.16 | 0.41 ± 0.05         | 135 ± 48 |

a. Diffusion time =  $\Delta\delta/3$  [ms].

Uncertainties indicate standard deviation.

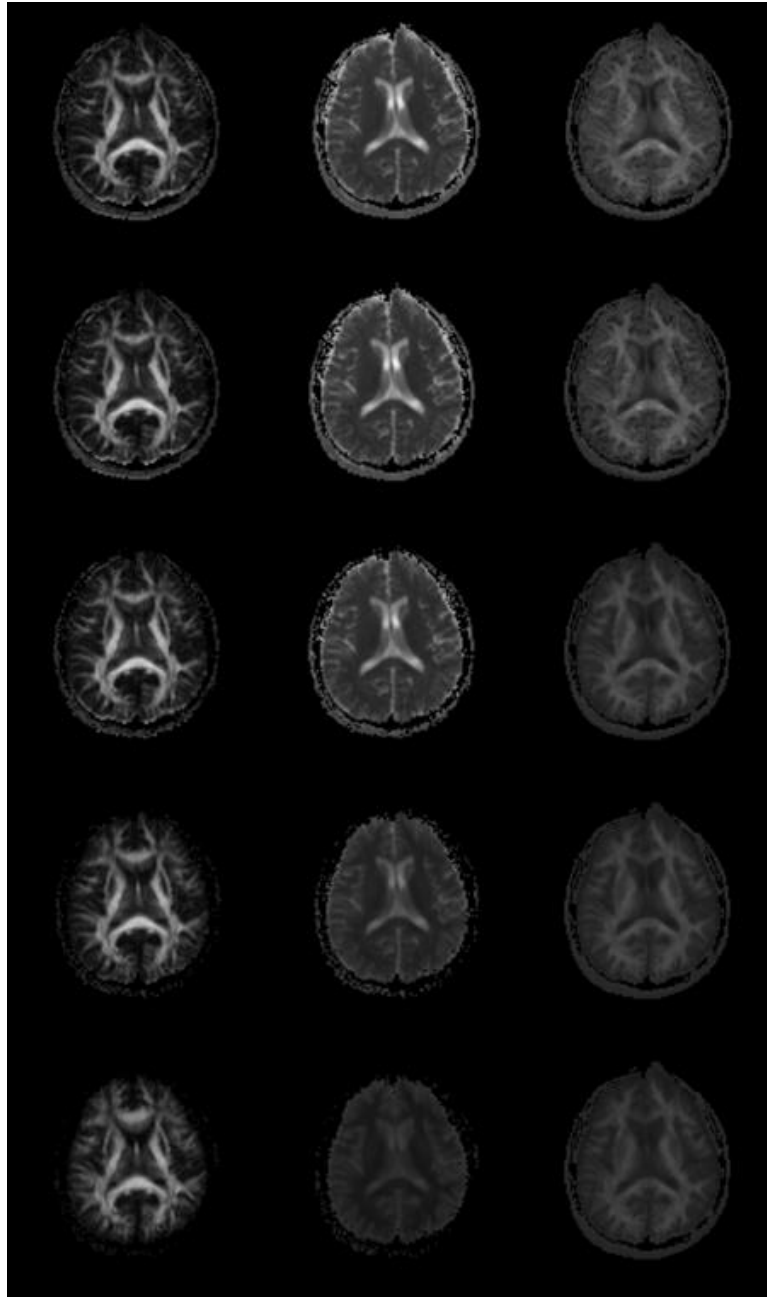


Fig. 4-2 Left to right columns, fractional anisotropy (FA), apparent diffusion coefficient (ADC), and mean diffusional kurtosis (DK) maps of the brain of a healthy volunteer.

Top row (Protocol 1): 0, 1000, and 2000 ( $\text{s}/\text{mm}^2$ ),

2nd row (Protocol 2): 0, 500, 1000, 1500, 2000, and 2500 ( $\text{s}/\text{mm}^2$ ),

3rd row (Protocol 3): 0, 500, 1000, 2000, 3000, and 5000 ( $\text{s}/\text{mm}^2$ ),

4th row (Protocol 4): 0, 1000, 3000, 5000, 6000, and 7000 ( $\text{s}/\text{mm}^2$ ),

5th row (Protocol 5): 0, 5500, 6000, 6500, 7000, and 7500 ( $\text{s}/\text{mm}^2$ )

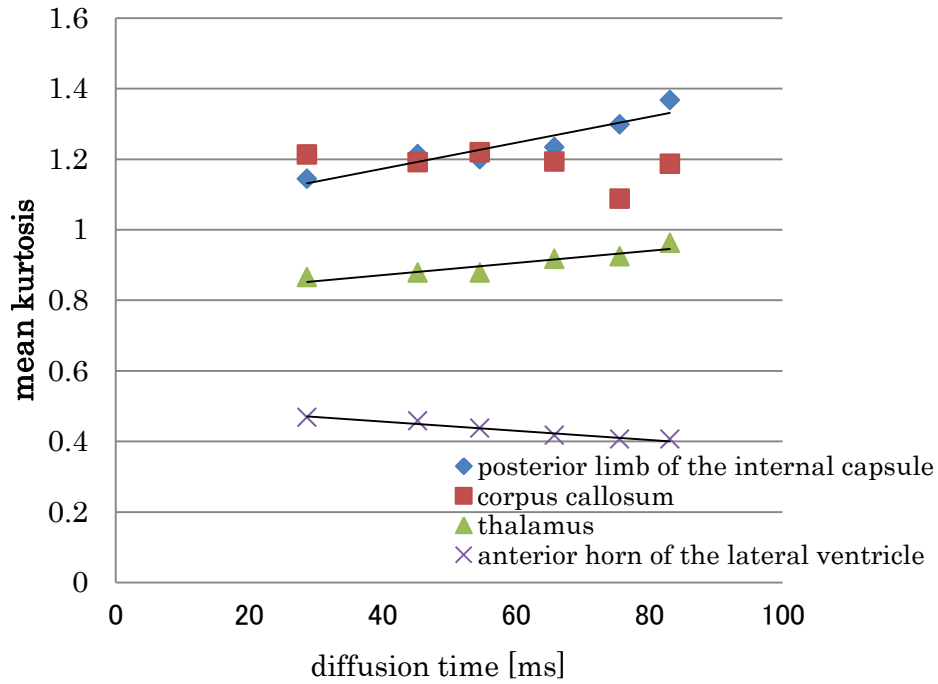


Fig. 4-3 Relationship between mean kurtosis (MK) and diffusion time in the posterior limb of the internal capsule (PLIC), corpus callosum (CC), thalamus, and anterior horn of the lateral ventricle. The solid lines represent the linear regression line between MK and diffusion time

#### 4.4 Discussion

##### Discussion 1.

It has been previously reported that the water signal decay of the human brain departs from the mono exponential behavior commonly assumed when ADC maps are generated in clinical practice, once the b-value range is extended above 6000 [s/mm<sup>2</sup>]<sup>30</sup>.

These results for the ADC maps were consistent with a previous study <sup>30)</sup>; the poor contrast between WM and GM was shown in Protocols 4 and 5 (Fig. 4-2). From Eq. (16), it has been shown that the value of the apparent diffusion kurtosis coefficient can be influenced by the ADC <sup>11)</sup>.

It is shown that one simulation using with use of typical parameters (ADC = 1 [ $\mu\text{m}^2/\text{ms}$ ], apparent kurtosis coefficient = 1) showed that the quadratic approximation would no longer be valid when the b value was 3000 [ $\text{s}/\text{mm}^2$ ] or larger. Therefore, the maximum b value should be limited to within about 3000 [ $\text{s}/\text{mm}^2$ ] <sup>11)</sup>. In this study for the MK maps, the poor contrast between WM and GM was shown in Protocols 3, 4, and 5 (Fig. 4-2).

It has been reported that the regional mean kurtosis values in the PLIC, in the body of the CC, and in the thalamus were  $1.23 \pm 0.09$ ,  $1.17 \pm 0.07$ , and  $0.86 \pm 0.07$ , respectively

<sup>31)</sup>. These results for Protocol 1 of the PLIC, CC, and thalamus were  $1.22 \pm 0.15$ ,  $1.04 \pm 0.13$ , and  $0.91 \pm 0.11$ , respectively. These results were consistent with a previous study as regional mean kurtosis value in the PLIC, in the body of the CC, and in the thalamus

<sup>31)</sup>. To scan DKI data for the whole brain in a clinically acceptable time, this study

support that three b values ( $b = 0, 1000, \text{ and } 2000 \text{ s/mm}^2$ ) may be powerful tool for evaluating neural tissue in vivo.

Discussion 2. It has previously been shown that for adequately measuring the MK, it is necessary to employ at least 15 different diffusion-encoding directions <sup>6)</sup>. However, another study reported that it might be sufficient to measure in only six diffusional directions in order to obtain a DK estimate, for example, in the evaluation of MS lesions <sup>32)</sup>.

This study focused on the SD of the MK value, and there was a remarkable difference in the SD of the MK values in the number of MPG directions. The difference in the SD of the MK values has influenced the signal loss or calculation errors due to MPG directions. These results indicate that the SD of the MK values was higher in 15 MPG directions than in 20 MPG directions and more. The MPG directions should be therefore number 20 or more for evaluation of the MK value.

Discussion 3. It has been previously reported that the mean diffusional kurtosis value in freely diffusing water molecules is theoretically zero <sup>6)</sup>. However, one study reported that the histograms of the MK values had peaks for CSF of approximately 0.45 <sup>33)</sup>.

Another study reported that pure CSF has an intrinsically low kurtosis due to flow effects <sup>34)</sup>.

This study assumed that the MK value of the CSF would be close to zero, and these results indicate this hypothesis. Because the MK values were significantly lower when we used longer diffusion times, this study expects longer diffusion times to be useful for DKI. However, diffusion in the CSF is not a Gaussian distribution, because of the flow effect, choroid plexus, and membranes.

There are some limitations to this study. First, this study population was small in number. Second, the voxel size in this study was  $3 \times 3 \times 3 \text{ mm}^3$ . Third, it is known that the kurtosis values are influenced by other factors, such as noise, motion, and imaging artifacts <sup>12)</sup>.

## 4.5 Conclusion

From the above results, this study considered that following imaging parameters were suitable for clinical use: TR/TE 7437/70ms; slice thickness 3mm;  $3 \times 3 \text{mm}$  resolution; MPG directions 20; b value 0, 1000, 2000[s/mm<sup>2</sup>];  $\Delta/\delta$  45.3 / 13.3ms.

# Chapter 5. Effects of Diffusion Time on Diffusion Quantification of Diffusional Kurtosis Imaging

## 5.1 Introduction

Diffusional kurtosis imaging (DKI) is a new technique based on non-Gaussian water diffusion analysis. Because water diffusion in the brain is restricted (non-Gaussian), DKI provides more precise diffusional information derived from the tissue microstructure than in conventional diffusion analysis such as diffusion tensor imaging (DTI, assuming Gaussian) <sup>6), 11), 12)</sup>. There are few reports of the imaging parameters of DKI <sup>11), 12)</sup> compared with those of DTI <sup>13)-15)</sup>. In DTI, previous studies reported that the diffusion quantification of white matter might be influenced by TE and diffusion time <sup>28)</sup>. In our previous study, we have shown that the relationships between mean kurtosis metrics and diffusion time in the white matter, gray matter, and, cerebrospinal fluid, that work did not give results for axial and radial diffusional kurtosis metrics <sup>35)</sup>. To examine the relationship between the diffusional kurtosis metrics and diffusion time, this study compared different acquisition in human studies.

## 5.2 Materials and Methods

Four normal healthy subjects (age range 21–25 years, mean age 22.8 years) participated in the study. This study was approved by the institutional review board of Tokyo Metropolitan University (No. 14053) and Juntendo University School of Medicine (No. 351). Written informed consent was obtained from all participants and their relatives. All DKI data were acquired on a clinical 3T-MRI scanner (Philips Medical Systems, Best, The Netherlands) with use of protocols as follows:

TR/TE 5000/56-97ms; slice thickness 3mm; resolution 3×3 mm; 3 b values (0, 1000, and 2000 s/mm<sup>2</sup>) with diffusion encoding in 30 directions for every b value. Gradient length ( $\delta$ ) was 10, 10.8, 12, 13.3, and 17.9 ms and the time between the two leading edges of diffusion gradient ( $\Delta$ ) was 28.7, 45.3, 54.6, 65.8 and 75.6 ms.  $\delta/\Delta$  diffusion time ( $\Delta-\delta/3$ ), 17.9/ 28.7/ 22.7, 13.3/ 45.3/ 40.9, 12.0/ 54.6/ 50.6, 10.8/ 65.8/ 62.2, 10.0/ 75.6/ 72.3 ms. The number of signals averaged was set at 1, 2, 2, 2, and 3, respectively.

All data were calculated for all diffusion metric maps such as FA, ADC, axial diffusivity, radial diffusivity (using b = 0, 1000 s/mm<sup>2</sup>), mean kurtosis (MK), axial kurtosis (AK), and radial kurtosis (RK) (using b = 0, 1000, and 2000 s/mm<sup>2</sup>) with the software dTV.13k

<sup>28</sup>). The volumes of interest (VOIs) were placed on the PLIC, CC, thalamus, and terminal zone of myelination (peritrigonal white matter) <sup>36</sup>). The size of VOIs was 19 voxels. In studying the VOIs, the VOIs were saved and used for every subject and every protocol.

Statistical analysis was performed with Scientific Package for Social Sciences, version 20 (SPSS, Chicago, Illinois). This study used Pearson correlation to investigate the relationships between all diffusion metrics and diffusion time.

### 5.3 Results

The FA values were significantly higher in the PLIC ( $p=0.013$ ,  $r=0.544$ ) with use of a longer diffusion time. No significant differences were found between the ADC values and diffusion time. The axial diffusivity values were significantly higher with use of a longer diffusion time in the PLIC ( $p=0.031$ ,  $r=0.484$ ) and the peritrigonal white matter ( $p=0.036$ ,  $r=0.470$ ). The radial diffusivity values were significantly lower in the PLIC ( $p=0.002$ ,  $r=-0.641$ ) with use of a longer diffusion time. The MK values were significantly lower with use of a longer diffusion time in the peritrigonal white matter ( $p=0.033$ ,  $r=-0.479$ ). The RK values were significantly higher with use of a longer diffusion time in the PLIC ( $p=0.032$ ,  $r=0.481$ ).

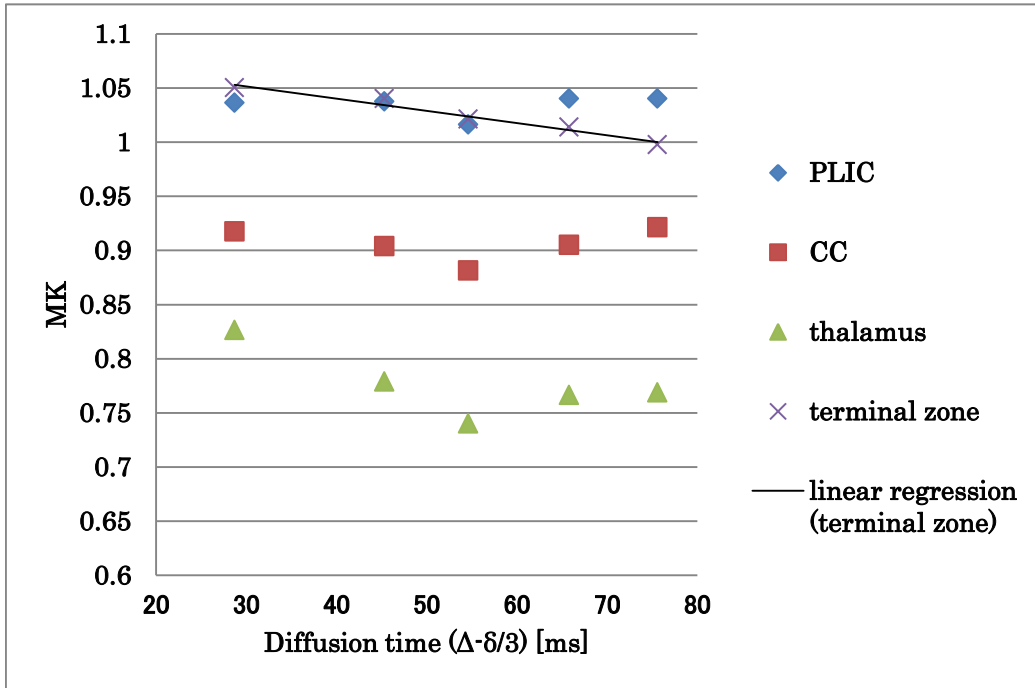


Fig. 5-1 Relationship between mean kurtosis and diffusion time in the posterior limb of the internal capsule, corpus callosum, thalamus, and terminal zone of myelination (peritrigonal white matter). The solid lines represent the linear regression line between mean kurtosis and diffusion time in the terminal zone.

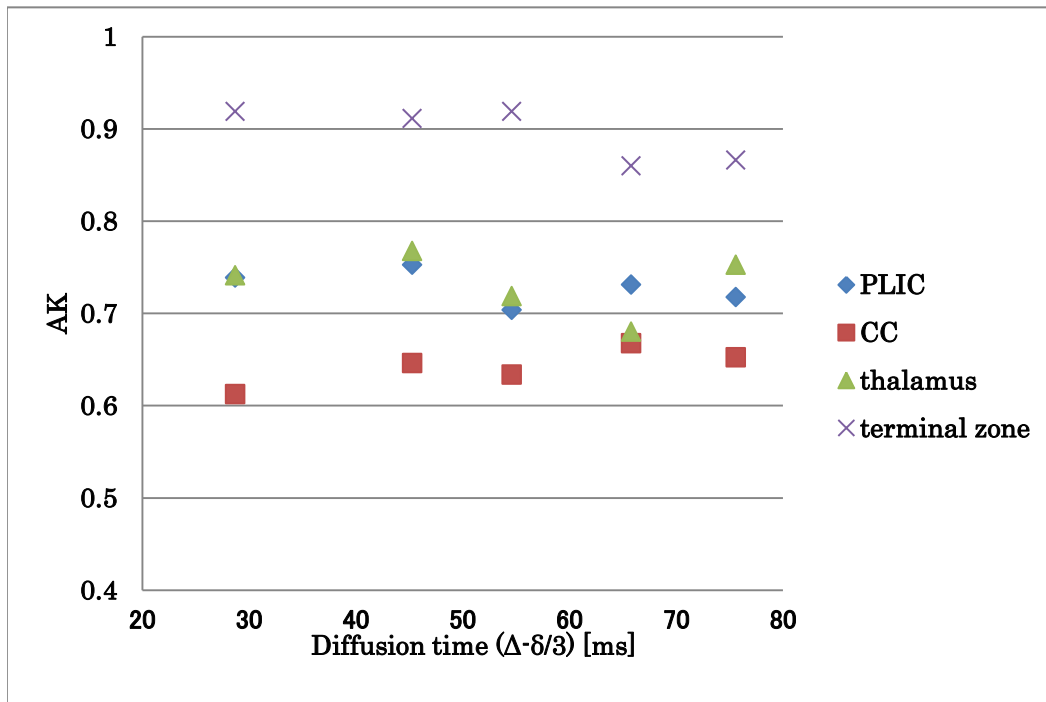


Fig. 5-2. Relationship between axial kurtosis and diffusion time in the posterior limb of the internal capsule, corpus callosum, thalamus, and terminal zone of myelination (peritrigonal white matter).

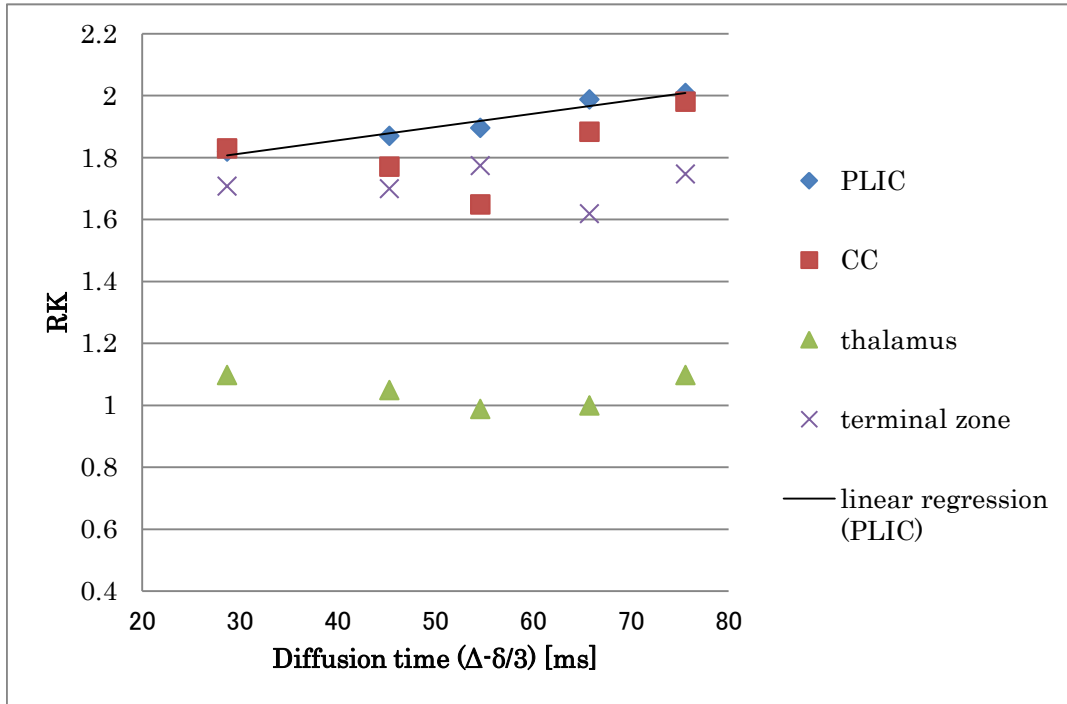


Fig. 5-3 Relationship between radial kurtosis and diffusion time in the posterior limb of the internal capsule, corpus callosum, thalamus, and terminal zone of myelination (peritrigonal white matter). The solid lines represent the linear regression line between radial kurtosis and diffusion time in the posterior limb of the internal capsule.

## 5.4 Discussion

This study represents the first evaluation of the relationships between the diffusional kurtosis metrics and diffusion time in human brain in vivo. This study indicates that the diffusional kurtosis metrics can be influenced by the diffusion time.

It has been previously reported that the FA and axial diffusivity demonstrated positive correlation with TE in the PLIC <sup>29)</sup>. The increase of the axial diffusivity resulted in the absence of cellular boundaries. The decrease of the radial diffusivity might be observed because of the increased interaction of water molecules with the cellular boundaries. The increase of the axial diffusivity and the decrease of the radial diffusivity could contribute to the increase of FA by increasing diffusion time <sup>29)</sup>. These results for the FA and axial diffusivity were consistent with a previous study. In the PLIC, the increase of the RK values reflects the restriction of axons (more diffusion barriers) when we used a longer diffusion time.

The peritrigonal zone of the lateral ventricles is described by persistent high signal intensity on T2 weighted images. It is assumed that the persistence of T2 high signal intensity as the expression of an absence of myelination. The T2 high signal intensity in

the peritrigonal zones could be partially referred to perivascular spaces <sup>36</sup>). The MK values were negatively correlated with diffusion time in the peritrigonal white matter.

In the terminal zone of myelination (peritrigonal white matter), the decrease of the MK values reflects unrestricted diffusion (less diffusion barriers), when we used a longer diffusion time.

## 5.5 Conclusion

The results suggest that diffusion quantification of the diffusional kurtosis metrics might be influenced by diffusion time. This knowledge may be helpful for clinical research studies, for instance longitudinal studies.

## Chapter6. Summary of the study

This study focuses on the DKI technique for evaluation of diffusional kurtosis metrics and diffusion time. This study shows that the RK values were positively correlated with diffusion time in the PLIC and the MK values were negatively correlated with diffusion time in the peritrigonal white matter when we used a longer diffusion time.

There are some limitations to this study. First, the subjects in this study were small in number. Second, the voxel size in this study was  $3\times 3\times 3$  mm<sup>3</sup>. Third, it is known that the kurtosis values are influenced by other factors, such as noise, motion, and imaging artifacts.

In summary, this study shows that the diffusional kurtosis metrics can be influenced by the diffusion time. This result may be helpful for future research of DKI, to evaluate the effect of diffusion time.

## References

- 1) Warach S, Chien D, Li W et al. : Fast magnetic resonance diffusion-weighted imaging of acute human stroke. *Neurology* 42 (9) : 1717-1723, 1992.
- 2) Mintorovitch J, Yang GY, Shimizu H et al. : Diffusion-weighted magnetic resonance imaging of acute focal cerebral ischemia: comparison of signal intensity with changes in brain water and Na<sup>+</sup>, K<sup>(+)</sup>-ATPase activity. *J Cereb Blood Flow Metab* 14 (2) : 332-336, 1994.
- 3) Beaulieu C, Does MD, Allen PS : Changes in water diffusion due to Wallerian degeneration in peripheral nerve. *Magn Reson Med* 36 : 627-631, 1996.
- 4) Fung SH, Roccatagliata L, Schaefer PW et al. : MR Diffusion Imaging in Ischemic Stroke. *Neuroimage* 21 : 345-377, 2011.
- 5) Cheung MM, Hui ES, Wu EX et al. : Does diffusion kurtosis imaging lead to better neural tissue characterization? A rodent brain maturation study. *NeuroImage* 45 : 386-392, 2009.
- 6) Jensen JH, Helpern JA, Kaczynski K et al. : Diffusional Kurtosis Imaging : The

Quantification of Non-Gaussian Water Diffusion by Means of Magnetic Resonance Imaging. *Magn Reson Med* 53 : 1432-40, 2005.

7) Assaf Y, Ben-Bashat D, Cohen T et al. : High b value q-Space Analyzed Diffusion-Weighted MRI : Application to Multiple Sclerosis. *Magnetic Resonance in Medicine* 47 : 115-126, 2002.

8) Raab P, Hattingen E, Lanfermann H et al. : Cerebral Gliomas: Diffusional kurtosis Imaging Analysis of Microstructural Differences. *Radiology* 254 : 876-881, 2010.

9) Wang JJ, Lin WY, Wai WW et al. : Parkinson Disease : Diagnostic Utility of Diffusion Kurtosis Imaging. *Radiology* 261 : 210-217, 2011.

10) Helpert JA, Adisetiyo V, Jensen JH et al. : Preliminary Evidence of Altered Gray and White Matter Microstructural Development in the Frontal Lobe of Adolescents with Attention-Deficit Hyperactivity Disorder : A Diffusional Kurtosis Imaging Study. *JMRI* 33 : 17-23, 2011.

11) Lu H, Jensen JH, Helpert JA : Three-dimensional characterization of non-gaussian water diffusion in humans using diffusion kurtosis imaging. *NMR Biomed* 19 : 236-247, 2006.

- 12) Jensen JH, Helpert JA : MRI quantification of non-Gaussian water diffusion by kurtosis analysis. *NMR Biomed* 23 : 698-710, 2010.
- 13) Correia MM, Carpenter TA, Williams GB : Looking for the optimal DTI acquisition scheme given a maximum scan time: are more b values a waste of time?. *Magnetic resonance Imaging* 27 : 163-175, 2009.
- 14) Ogura A, Hayakawa K, Miyati T, Maeda F : Imaging Parameter effects in apparent diffusion coefficient determination of magnetic resonance imaging. *European Journal of Radiology* 77 : 185-188, 2011.
- 15) Ozaki M, Ogura A, Takizawa O et al : Influence of Imaging Parameters on the Measurement of Apparent Diffusion Coefficient. *Japanese Journal of Radiological Technology* 63 : 91-96, 2007.
- 16) Stejskal EO, Tanner JE : Spin diffusion measurement: spin echoes in the presence of a time dependent field gradient. *J Chem Phys* 42 : 228-292, 1965.
- 17) Hashemi RH, Bradley WG, Lisanti CJ : MRI the Basics second edition : 263-270, LIPPINCOTT WILLIAMS & WILKINS, 2004.
- 18) Jones DK : Diffusion MRI Theory, Methods, and Application : 57-124, Oxford University Press,

2011

19) Melthem ER, Mori S, Zijl V et al. : Diffusion Tensor MR Imaging of the Brain and White Matter Tractography. *AJR* 178 : 3-16, 2002.

20) Oishi K, Faria A, Mori S et al. : MRI Atlas of Human White Matter second edition : 1-28, ELSEVIER ACADEMIC PRESS, 2011.

21) Qi L, Han D, Wu EX et al. : Principal invariants and inherent parameters of diffusion kurtosis tensors. *Journal of Mathematical Analysis and Applications* 349 : 165-180, 2009.

22) Masutani Y, Aoki S, Otomo K et al. : MR diffusion tensor imaging: recent advance and new techniques for diffusion tensor visualization. *European Journal of Radiology* 46 : 53-66, 2003.

23) Hyvarinen A, Karhunen J, Oja E : INDEPENDENT COMPONENT ANALYSIS : 19-42, WILEY-INTERSCIENCE , 2001.

24) Assaf Y, Mayk A, Cohen Y et al. : Hypertension and neuronal degeneration in excised rat spinal cord studied by high-b value q-space diffusion magnetic resonance imaging. *Experimental Neurology* 184 : 726-736, 2003.

- 25) Hori M, Fukunaga I, Masutani Y, et al. : Visualizing non-Gaussian diffusion: clinical application of q-space imaging and diffusional kurtosis imaging of the brain and spine. *Magn Reson Med Sci* 11(4) : 221–33, 2012.
- 26) Hori M, Fukunaga I, Masutani Y, et al. : New diffusion metrics for spondylotic myelopathy at an early clinical stage. *Eur Radiol* 22 : 1797–802, 2012.
- 27) Jones DK, Horsfield MA, and Simmons A : Optimal Strategies for Measuring Diffusion in Anisotropic Systems by Magnetic Resonance Imaging. *Magnetic Resonance in Medicine* 42 : 515-525, 1999.
- 28) Masutani Y, Aoki S : Fast and Robust Estimation of Diffusional Kurtosis Imaging (DKI) Parameters by General Closed-form Expressions and their Extensions. *Magn Reson Med Sci* 13(2) : 97–115, 2014.
- 29) Qin W, Yu CS, Li KC, et al. : Effects of echo time on diffusion quantification of brain white matter at 1.5 T and 3.0 T. *Magn Reson Med* 61 : 755–60, 2009.
- 30) Mulkern RV, Zengingonul HP, Maier SE, et al. : Multi-component apparent diffusion coefficients in human brain: relationship to spin-lattice relaxation. *Magn Reson Med* 44 : 292–300, 2000.

31) Laätt J, Nilsson M, and Johansson M, et al. : Regional values of diffusional kurtosis estimates in the healthy brain. JMRI 2012. doi:10.1002/jmri.23857.

32) Laätt J, Nilsson M, Brockstedt S, et al. : In vivo visualization of displacement-distribution-derived parameters in q-space imaging. Magn Reson Imaging 26 : 77–87, 2008.

33) Falangola MF, Jensen JH, Helpert JA, et al. : Age-related nongaussian diffusion patterns in the prefrontal brain. JMRI 28 : 1345–50, 2008.

34) Yang AW, Jensen JH, Helpert JA, et al. : Effects of cerebral spinal fluid suppression for diffusional kurtosis imaging. JMRI 37 : 365–71, 2013.

35) Fukunaga I, Hori M, Masutani Y, et al. : Effects of diffusional kurtosis imaging parameters on diffusion quantification. Radiol Phys Technol  
DOI 10.1007/s12194-013-0206-5 2013.

36) Parazzini C, Baldoli C, Scotti G, et al. : Terminal Zones of Myelination: MR Evaluation of Children Aged 20-40 Months. AJNR 23 : 1669-1673, 2002

## Acknowledgements

I would like to show my greatest appreciation to Atsushi Senoo, associate professor of Tokyo Metropolitan University, for useful advice and constant encouragement.

I would like to express my appreciation to Tomokazu Numano, associate professor of Tokyo Metropolitan University, for invaluable comments.

I would like to show my appreciation to Izumi Ogura, professor of Tokyo Metropolitan University, for useful suggestions.

I would like to express the deepest appreciation to Dr. Shigeki Aoki, professor of Juntendo University School of Medicine, for valuable discussion and helpful comments.

I would like to express my gratitude to Dr. Masaaki Hori, associate professor of Juntendo University School of Medicine, for valuable comments and helpful suggestions.

I am deeply grateful to Yoshitaka Masutani, professor of Hiroshima City University, for help with technical support and incisive comments.

I owe my deepest gratitude to Yuriko Suzuki, Philips Electronics Japan, for technical

support.

I would like to thank Nozomi Hamasaki, Shuji Sato, Fumitaka Kumagai, and Haruyoshi Hoshito, Juntendo University School of Medicine, for helpful advice and fruitful discussion.

The study was supported in part by a Grant-in-Aid for Scientific Research on Innovative Areas (Comprehensive Brain Science Network) from the Ministry of Education, Culture, Sports, Science, and Technology of Japan (MEXT). This study was also supported in part by a MEXT-Supported Program for the Strategic Research Foundation at Private Universities (S1101008), 2011–2015.